CMLS, Cell. Mol. Life Sci. 62 (2005) 227–238
1420-682X/05/020227-12
DOI 10.1007/s00018-004-4413-4

CMLS Cellular and Molecular Life Sciences

Research Article

Compensatory caspase activation in MPP$^+$-induced cell death in dopaminergic neurons

J. L. Y. Chee [a], X. L. Guan [a], J. Y. Lee [a], B. Dong [a], S. M. Leong [a], E. H. Ong [a], A. K. F. Liou [b] and T. M. Lim [a, *]

[a] Department of Biological Sciences, Faculty of Science, National University of Singapore, 14 Science Drive 4 117542 Singapore, e-mail: dbsltm@nus.edu.sg
[b] Institute of Neurodegenerative Disorders, University of Pittsburgh School of Medicine, Pittsburgh Pennsylvania 15261 (USA)

Received 20 September 2004; received after revision 5 November 2004; accepted 22 November 2004

Abstract. Many have hypothesized that cell death in Parkinson's disease is via apoptosis and, specifically, by the mitochondrial-mediated apoptotic pathway. We tested this hypothesis using a mouse dopaminergic cell line of mesencephalic origin, MN9D, challenged with the Parkinsonism-causing neurotoxin MPP$^+$ (1-methyl-4-phenylpyridinium ion). Apoptosis was the main mode of cell death when the cells were subjected to MPP$^+$ treatment under serum-free conditions for 24 h. Caspase-3 and caspase-9, however, were not activated, thus indicating the existence of alternate or compensatory cell death pathway(s) in dopaminergic neuronal cells. Using caspase inhibitors, we demonstrated that these pathways involve caspase-2, -8, -6 and -7. A time-course study indicated that activation of caspase-2 and -8 occurred upstream of caspase-6 and caspase-7. Upon MPP$^+$ challenge, the apoptosis-inducing factor was translocated from the mitochondria into the MN9D cytosol and nucleus. These results suggest the existence of alternative apoptotic pathways in dopaminergic neurons.

Key words. Caspase; AIF; apoptosis; cytochrome c; dopaminergic neuron; neurotoxin; Parkinson's disease.

Introduction

The recent findings of gene products responsible for familial forms of Parkinson's disease (PD) have provided significant insights into PD pathogenesis. These studies point toward the dysfunction of the ubiquitin-proteasome system (UPS) as an underlying mechanism responsible for dopaminergic cell death in PD [1–3]. However, the majority of PD cases are sporadic and their etiology remains poorly understood. Major biochemical processes such as oxidative stress and mitochondrial dysfunction are implied. Of the several hypotheses proposed, many share the central theme of stress-activated signaling and apoptotic pathways [4–9].

Apoptosis has been implicated as the main process responsible for the death of dopaminergic neurons in PD since DNA fragmentation was observed, using the 3′-end terminal staining of DNA (TUNEL method), in the substantia nigra of PD patients [10]. A similar approach was also applied to demonstrate the possible involvement of apoptosis in idiopathic PD cases [11]. Recent studies have focused on identifying the main players involved in the apoptotic process that selectively cause the loss of the midbrain dopaminergic neurons [5, 12]. However, as a result of methodological limitations and the inappropriate imposition of narrow criteria for the recognition of apoptosis, debate has surfaced as to whether apoptosis indeed contributes to neuronal loss in PD [9].

Among the 12 caspases characterized in mammals, caspase-3 has been associated with PD neuronal cell death [4, 13, 14]. Caspase-3 is activated by upstream caspase-9,

* Corresponding author.

whose activation in turn is dependent on the release of cytochrome *c* from mitochondria and the formation of the apoptosome [15, 16]. The release of cytochorme *c* could be due to physical disruption of the mitochondrial outer membrane through a phenomenon known as the mitochondrial membrane permeability transition (MPT) [7, 17]. Mitochondria also contain the apoptosis-inducing factor (AIF) which, when released, leads to the activation of caspases [18], and when translocated into the nucleus induces caspase-independent DNA fragmentation [19].

While the release of pro-apoptotic mitochondrial proteins and their redistribution to the cytosol and nucleus during cell death are well documented [7, 20], many studies have shown that the activation and regulation of caspase activity is complicated, involving several feedback loops and compensatory mechanisms [21, 22]. Additionally, the phosphorylation of p38 MAPK induced by oxidative stress was demonstrated to be linked to the activation of both caspase-8- and -9-mediated apoptotic pathways in dopaminergic neurons [23]. The unfolded protein response (UPR) is also involved in cell death triggered by the neurotoxins, 6-hydroxydopamine and MPP^+ [24]. Such observations highlight the need to further dissect the neuronal death pathway to facilitate understanding of PD and development of therapeutic strategies.

In this study, we employed the dopaminergic cell model, MN9D [25, 26], to study cell death induced by the administration of 1-methyl-4-phenylpyridinium (MPP^+), the active ion of the Parkinson-inducing neurotoxin 1-methyl-4-phenyl-1,2,3,6-tetrahydropyride (MPTP) [27]. The caspases involved were first identified and then their sequence of activation mapped. Apoptosis was correlated with the release of AIF and cytochrome *c*. Our results agreed with recent reports which showed that caspase-3 was not involved in the process [12, 24]. Importantly, we demonstrate the existence of compensatory mechanisms involving AIF, caspase-2, -8, -6 and -7 to mediate cell death when dopaminergic neurons were challenged with MPP^+.

Materials and Methods

Routine cell culture and characterization

The MN9D cell is a mouse dopaminergic neuronal cell line derived from the fusion of rostral mesencephalic neurons from embryonic C57BL/6J mice with N18TG2 neuroblastoma cells [25]. MN9D was deemed suitable in this study because it is dopaminergic and neuronal in nature – a fundamental feature for cell lines used as PD models. In addition, it is of mesencephalic origin – a feature absent in other cell models used currently. MN9D cells were routinely cultured in Primaria-coated petri dishes (BD Bioscience) or Corning petri dishes in Dulbecco's MEM (DMEM) (NUMI) containing 10% fetal bovine serum (Hyclone) and 1% v/v penicillin-streptomycin (Sigma). The MN9D cells were from Dr J. Chen of the University of Pittsburgh and were used with permission from Dr A. Heller of the University of Chicago. The cells were characterized to be dopaminergic using Western blot analysis of the cell extract with antibodies against tyrosine hydroxylase (TH) and dopamine transporter (DAT). Immunocytochemistry using TH antibodies conjugated with HRP was also conducted to ascertain the cellular characteristics. We also determined dopamine in the MN9D cell lysate and in the cell culture medium using a multi-wall carbon nanotube electrode [28] connected to a CHI 660A electrochemical workstation (CH Instruments). Dopamine was extracted using the ion-pair extraction technique [29]. The detection was based on the oxidation of dopamine to dopaminequinone that generates cyclic voltammetry signals. The samples tested were compared with a set of standard dopamine solutions and the negative controls were N2a and HeLa cell lysates and their respective culture medium.

MPP^+ treatment

MN9D cells were seeded at 2×10^6 per well and cultured in serum-supplemented medium to approximately 80% confluence before any treatment. The optimum concentration of MPP^+ required for inducing maximal cell death under serum-free conditions was determined by treating the MN9D cells with 25 µM, 50 µM, 100 µM, 500 µM or 1 mM MPP^+ in serum-free medium for 24 h. The experiment was performed in quadruplicate. Cell viability was assessed using a tetrazolium dye (MTT: dimethylthiazol-diphenyltetrazolium bromide) assay. From the data, the dosage of 500 µM was chosen for subsequent experiments because higher dosage did not cause more cell death.

Acridine orange/ethidium bromide staining of MN9D cells

MN9D cells were harvested and 2 µl dye mix [100 µg/ml each of acridine orange and ethidium bromide in phosphate buffered saline (PBS)] was added to 50 µl cell suspension. An aliquot (10 µl) of the cell suspension was transferred to a microscope slide and observed under a fluorescence microscope (Olympus BX60) with an absorption wavelength of 300–400 nm and emission wavelength of 410–550 nm. Assessment of apoptotic versus necrotic cells was determined by visualization of the color and the state of the nucleus. The cells (at least 100 cells per sampling) were scored into four categories: live non-apoptotic (green nuclei, normal distribution of chromatin), live apoptotic (green nuclei, condensed chromatin), dead non-apoptotic/necrotic (orange nuclei, normal distribution of chromatin) and dead apoptotic (orange nuclei, condensed chromatin). Apoptotic cells were

quantified as a percentage of the total number of cells counted.

Cytotoxicity detection assay

Lactate dehydrogenase (LDH) activity was assayed using a cytotoxicity detection kit (Roche). Briefly, culture medium was harvested and centrifuged at 80 g for 5 min before assaying according to the manufacturer's instruction. The release of LDH reduced the tetrazolium salt to a red-colored formazan salt. The amount of formazan, which correlated directly with the amount of LDH activity, was quantified by absorbance at a wavelength of 490 nm. Data were expressed as a percentage of control cells not treated with MPP^+.

Cell inhibition studies

MN9D cells were cultured to 80% confluence in serum-supplemented medium and then exposed to inhibitors of caspase-2 (Z-VDVAD-FMK), caspase-3 (Z-DEVD-FMK), caspase-6 (Z-VEID-FMK), caspase-8 (Z-IETD-FMK), caspase-9 (Z-LEHD-FMK) (all caspase inhibitors were from Calbiochem), or wortmannin (Sigma), or SN50 (Calbiochem) for 24 h in the presence of 500 µM MPP^+ in serum-free medium. All chemicals used were dissolved in DMSO. The experiments were performed in triplicate and cell viability was assessed using the MTT assay.

Protein extraction

MN9D cells subjected to the various experimental conditions and the N2a cells (control) were washed with PBS to remove residual medium prior to protein extraction. Cell lysis buffer (100 mM HEPES pH 7.5, 5 mM $MgCl_2$, 150 mM NaCl, 1 mM EDTA, 1% Triton + 1% protease inhibitor cocktail) was then added and the cell lysate was extruded through a $27^1/_2$-G needle. The supernatant was collected after centrifuging the cell lysate at 13,000 rpm for 1 min, and stored at –20 °C. Protein concentrations of cell lysates were determined using the Bradford assay (BioRad).

Extraction of mitochondria and cytosolic protein fractions

Cells were lysed with pre-chilled MSHE buffer (0.21 M mannitol, 70 mM sucrose, 10 mM HEPES-KOH, pH 7.2, 1 mM EDTA, 1 mM EGTA, 0.15 mM spermine, 0.75 mM spermidine, 5 mM DTT, 1% protease inhibitor cocktail) and homogenized on ice using a Dounce homogenizer. After centrifugation at 500 g, 4 °C for 12 min, the supernatant was recentrifuged at 9500 g for 9 min at 4 °C to pellet the mitochondria. Supernatant containing the cytosolic fractions was removed and stored at –20 °C. Protein concentrations of lysates were determined using the Bradford protein assay.

Western blotting

The protein samples were first resolved in 12% SDS-PAGE gel and then transferred to nitrocellulose membranes. The blots for caspase-3 and -9 were blocked overnight in a blocking buffer (TBS containing 0.1% Tween-20 and 2% BSA) at 4 °C and then incubated with rabbit anti-mouse caspase-3 (1:1000) or caspase-9 (1:2000) for 1 h at room temperature (Cell Signaling). Blots for caspase-2, -6, -7, -8 and AIF were blocked with skim milk (TBS containing 0.1% Tween 20 and 5% low-fat skim milk) for 1 h. The blots were subsequently incubated with the respective primary antibodies [caspase-2 (1:1000) and caspase-8 (1:1000) (Santa Cruz); caspase-6 (1:1000) (Chemicon); caspase-7 (1:600) (Labvision); mouse anit-AIF (1:500; Santa Cruz); rabbit anti-cytochrome *c* (1:200; Clontech), mouse anti-COX I (1:1000; Molecular Probes) and mouse anti-actin (1:1000; Santa Cruz Biotechnology)] overnight at 4 °C. All the blots were washed with TBS-Tween (TBS containing 0.1% Tween-20) and then incubated with the secondary antibodys, anti-rabbit-HRP (1:2000; Santa Cruz), for 2 h at room temperature. Specific bands of interest were detected by developing with the enhanced chemiluminescent (ECL) kit (Pierce) and the signals were detected on Kodak CL-Xposure films.

Immunocytochemistry detection of AIF translocation

MN9D cells were cultured on poly-D-lysine-coated chamber slides. The cells were exposed to the experimental conditions followed by incubating in fresh serum-free medium containing 250 nM MitoTracker Red dye (Molecular Probes) at 37 °C to stain the mitochondria. The cells were first fixed with 3% paraformaldehyde dissolved in PBS, then blocked with blocking buffer (10% horse serum and 0.4% TritonX-100 in PBS) and washed once with a washing buffer (0.4% TritonX-100 in PBS) before incubating with 1:1000 dilution of AIF primary antibody (Santa Cruz Biotechnology) overnight at 4 °C. After washing and incubating with a probing buffer containing 1:100 dilution of secondary antibody (FITC-conjugated anti-goat; Chemicon), the cells were washed and observed using the Fluoview 500 Laser Scanning Confocal microscope (Olympus). Mitochondria were detected at an excitation and emission wavelength of 579 nm and 599 nm respectively, while AIF was detected at an excitation wavelength of 492 nm and an emission wavelength of 520 nm. The images were processed and edited using the Zeiss Image Browser software.

Statistics

Data provided are the mean ± SE. The one-way ANOVA and post hoc Student's t test were used to determine statistical significance between control and treated samples and values of $p < 0.05$ were considered statistically significant.

Results

Dopaminergic characteristics of MN9D cells

The dopaminergic characteristics of MN9D cells were validated using immunoblots of MN9D cell extracts against DAT and TH. Both TH (fig. 1A) and DAT (fig. 1B) proteins were detected in unchallenged and challenged cells but not in N2a, a non-dopaminergic neuroblastoma cell line. The MN9D dopaminergic property was also not affected by MPP^+ treatment. Most cells showed positive staining with TH immunocytochemistry (fig. 1C). Using electrochemical determination of dopamine with a multi-wall carbon nanotube electrode, we found that the dopamine level in the MN9D cell lysate was about three times that found in the MN9D cell medium. No dopamine was detected in the N2a and HeLa cells (data not shown). The dopaminergic characteristics of our MN9D cells were consistent with early reports stating that the parental cell line could synthesize, release and take up dopamine [25, 30]. MN9D cells have been used in several laboratories as a model for studying PD [12, 31–36] and are a useful system for investigating the specific roles of cell death pathways as well as to identify the nuclear/cytoplasmic components which participate in these pathways.

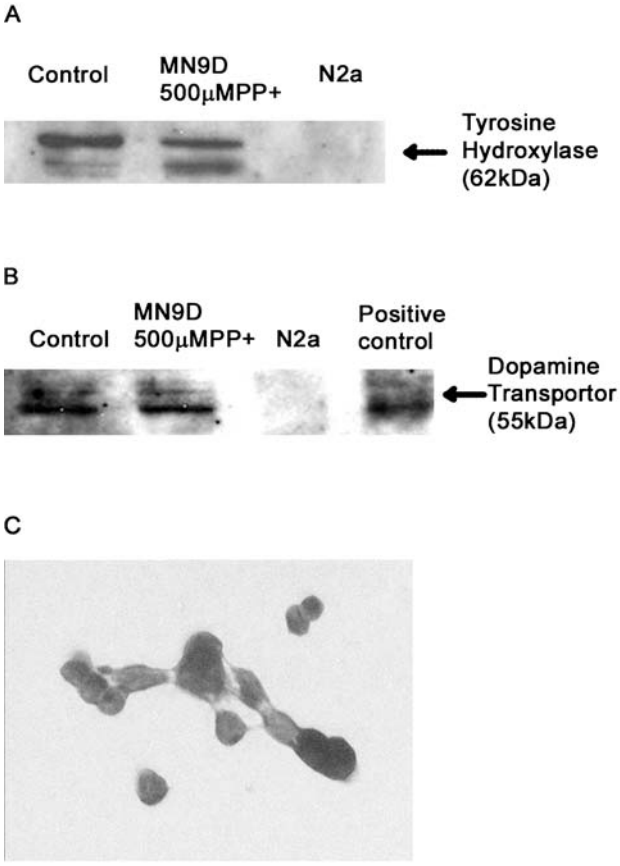

Figure 1. Dopaminergic characteristics of MN9D cells. Cells were treated with 500 μM MPP^+ for 24 h. Cytosolic proteins were separated by 12% SDS-PAGE and transferred to nitrocellulose membrane. Blots were immunolabeled with anti-tyrosine hydroxylase (*A*) and anti-dopamine transporter (*B*) antibodies. Detection of specific bands was achieved using enhanced chemiluminescence. (*C*) Immunocytochemistry showing MN9D cells stained with HRP-conjugated anti-tyrosine hydroxylase antibodies.

Apoptosis – the mode of cell death in MPP^+-challenged MN9D cells

The dosage response of MN9D cells to MPP^+ treatment over 24 h is shown in figure 2A. The optimum concentration of MPP^+ required for inducing maximal cell death at around 40% was found to be 500 μM. This was chosen as a standard dosage for further experiments since higher concentrations of MPP^+ did not increase cell death. This seemed to be the saturation point of MPP^+ toxicity and thus a good reference point to assess the cell death mechanisms involved under our experimental serum-free condition.

An LDH assay was used to detect necrotic cell death when MN9D cells were challenged with 500 μM MPP^+ (fig. 2B). There was no significant increase in the percentage of necrotic cell death with increasing concentrations of MPP^+ since the LDH production remained relatively constant with various levels of MPP^+. To further test for the presence of apoptotic characteristics, chromatin condensation was observed using acridine orange/ethidium bromide staining (fig. 2C). The results showed that MPP^+-challenged MN9D cells were mainly dying via apoptosis (fig. 2D).

Caspase-3 and -9 were not induced by MPP^+ despite cytochrome *c* release

MPP^+ is reported to induce mitochondria damage in cells [37, 38] resulting in the release of proapoptotic protein cytochrome *c* [39], thereby leading to the activation of caspases. The release of cytochrome *c* from the MN9D mitochondria was demonstrated in the subcellular fractionation and immunoblot analysis using anti-cytochrome *c* antibody (fig. 3A). Although a basal level of cytochrome *c* was detected in the cytosolic fraction even without MPP^+ treatment, this level increased significantly within the first 2 h of MPP^+ treatment without further changes thereafter. None of the cytosolic fractions was positive for cytochrome oxidase subunit I (COXI), a marker protein for the mitochondrial fraction, indicating that cytochrome *c* was indeed released into the cytosol after MPP^+ treatment and was not there due to membrane leakage during sample preparation. The blots were also probed with actin, an abundant cytosolic protein, to verify that each lane was loaded with equivalent amount of protein (fig. 3A). The induction of mitochondrial release of cytochrome *c* by MPP^+ has also been demonstrated [12].

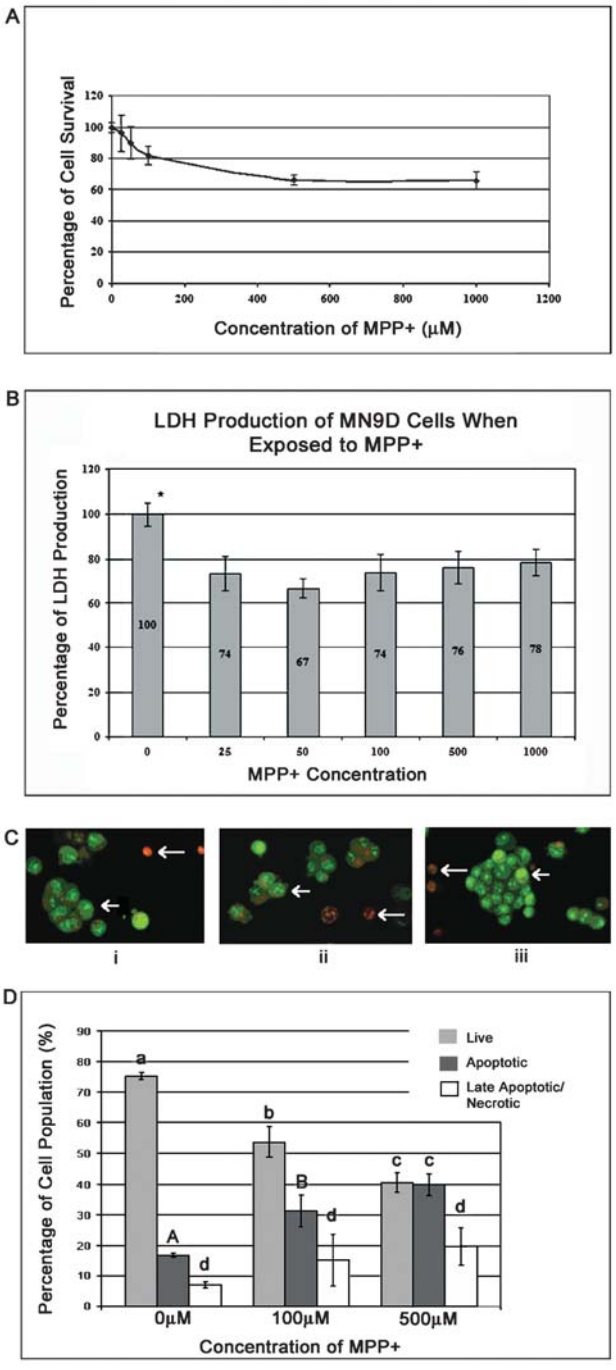

Figure 2. MPP+-induced cell death in MN9D cells. (*A*) Cells were treated with various concentrations of MPP+ to induce cell death. Cell viability after 24-h exposure to MPP+ was assessed using an MTT assay. (*B*) LDH quantification determined if the cells were dying via necrosis or apoptosis. Medium from treated cell cultures was harvested, and assayed as described. * denotes statistically significant values at $p < 0.05$. (*C*) Photomicrographs of MN9D cells stained with acridine orange and ethidium bromide after MPP+ treatment for 24 h: i, unchallenged MN9D cells; ii, MN9D cells challenged with 100 μM MPP+; iii, MN9D cells challenged with 500 μM MPP+. Long arrows indicate cells stained with ethidium bromide implying late apoptotics or necrosis while short arrows represent cells undergoing early apoptosis (×200 magnification). (*D*) Percentage of cells undergoing apoptosis/necrosis. Error bar superscripts that differ are statistically significant ($p < 0.05$).

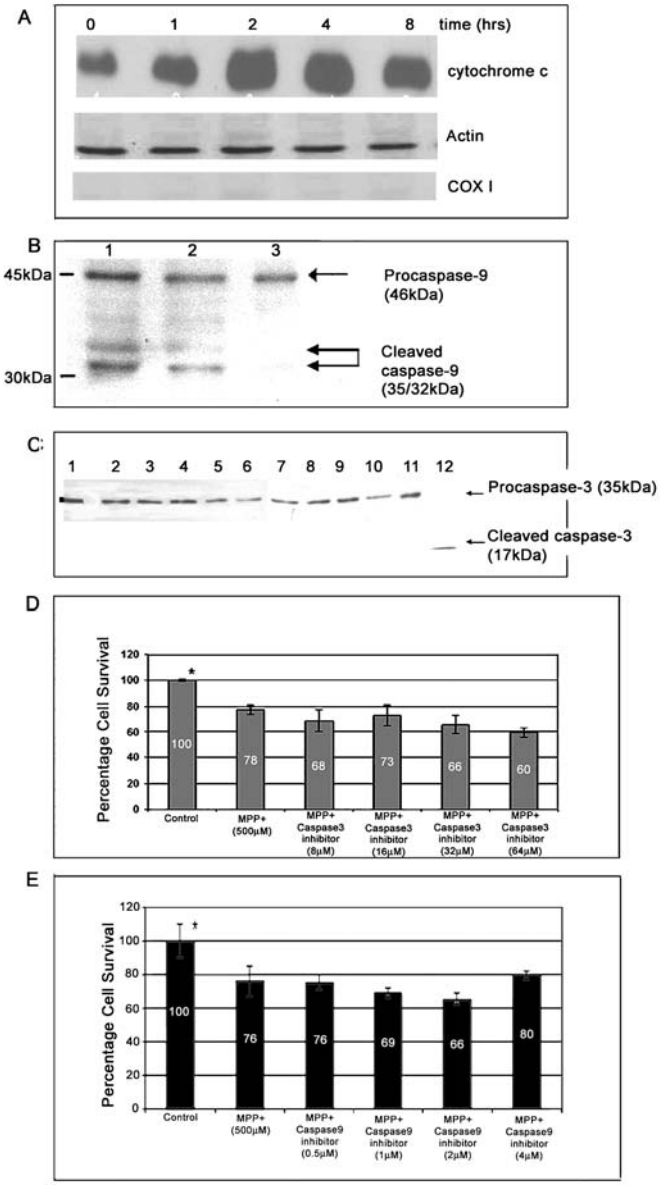

Figure 3. Detection of cytochrome *c* and caspase-3 and -9 in MPP+-treated MN9D cells. (*A*) Western blot analysis of AIF and cytochrome *c* in cytosolic fractions of MN9D cells challenged with 500 μM MPP+. Actin and COXI were probed to verify that equal amounts of protein were loaded in each lane, and to detect leakage of mitochondria membranes, respectively. Activation of caspase-9 and -3 was detected using antibodies that recognize both the pro- and cleaved forms. (*B*) Lane 1, MN9D cells unchallenged; lane 2, MN9D cells treated with MPP+ and Lane 3, N2a cells unchallenged. (*C*) Lane 1, unchallenged MN9D cells; lanes 2–9, cells challenged with MPP+ for 1, 2, 4, 8, 16, 24, 48 and 72 h, respectively; lane 10, N2a cell unchallenged; lane 11, MN9D cells treated with 3 μM rotenone for 24 h and lane 12, positive control for caspase-3. (*D, E*) Percentage cell survival of MPP+-treated MN9D cells in the presence of caspase-3 and -9 (*E*) inhibitors. Data represent the means from three independent experiments and error bars are ±1 SE (* $p < 0.05$).

To test whether the caspases involved in the mitochondrial-mediated apoptotic pathway were activated, extracts of unchallenged cells and MN9D cells challenged with MPP^+ were immunoblotted for the activation of both caspase-9 and its downstream partner caspase-3. Figure 3A shows the activation of caspase-9 and the presence of the two cleavage products of about 32–35 kDa, which were not detected in the negative control, N2a cells. Surprisingly, despite the fact that caspase-9 was activated constitutively there was no subsequent activation of the downstream caspase-3 during the course of MPP^+ treatment (fig. 3C). We also tested the activation of caspase-3 in MN9D cells challenged with 3 µM rotenone and, again, we did not detect caspase-3 activation (fig. 3C, lane 11). Inhibition studies against caspase-9 and caspase-3 further confirmed the results because the inhibition of these two caspases did not rescue the MPP^+-challenged cells from cell death (Fig. 3D, E). These results present the possibility of alternate apoptotic pathway(s) in MN9D cells induced by MPP^+, which may be either caspase independent or involve some compensatory mechanisms with other caspases.

Involvement of XIAP in the blockage of the mitochondria-dependent apoptotic cell death

With the demonstration that the caspase-9/3 pathway in the MN9D cells had been blocked, a prime candidate to such a phenomenon was X chromosome-linked inhibitor of apoptosis protein (XIAP). Studies [40, 41] have shown the ability of XIAP to bind to caspase-3 and activated caspase-9, hence blocking the caspase-9/3 apoptotic pathway. The expression of XIAP has been demonstrated to depend on the activation of NF-κB transcription factor [42]. SN50, an inhibitor of NF-κB phosphorylation was used to block the activation of NF-κB, and hence the expression of XIAP. The effect of SN50 on the viability of unchallenged as well as MPP^+-challenged MN9D cells was tested and assessed via MTT assay. As shown in figure 4, the inhibition of NF-κB activation led to a decrease in cell viability of almost 20%. Statistical calculations using Student's t test demonstrated that the decrease in cell viability was significant when the dosage of SN50 was 3 and 9 µM. The results were consistent with the proposed hypothesis that XIAP is involved in the blockage of the caspase-9/3 apoptotic pathway. The LDH assay done on the same set of cells showed that there was no increase in the amount of necrotic cell death. The results further supported the hypothesis that the death of MN9D cells due to MPP^+ toxicity was via the apoptotic pathway.

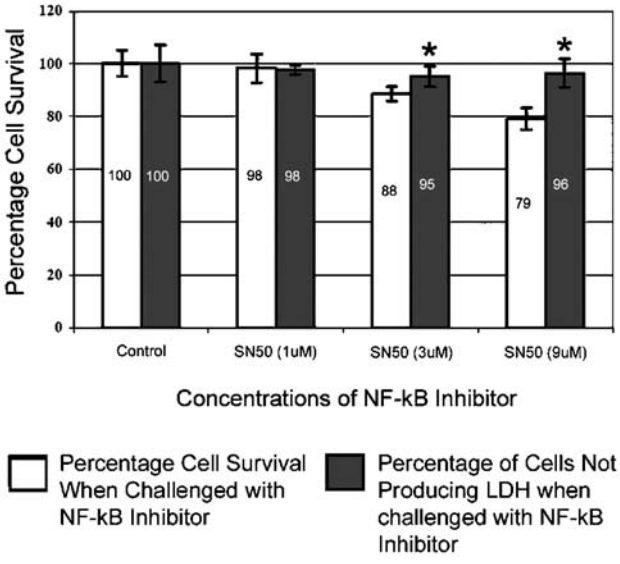

Figure 4. Percentage survival of MN9D cells challenged with MPP^+ in response to NF-κB inhibitor (SN50). Cells were treated with 500 µM MPP^+ for 24 h in the presence of SN50 at concentrations of 0, 1, 3 and 9 µM, cell viability was assayed using an MTT assay after treatment and was expressed as a percentage of control cells. Data represent the mean ± SE from three independent experiments (* $p < 0.05$).

AIF was released from the mitochondria upon MPP^+ challenge

AIF exists in two forms – the pro-form with a molecular size of 67 kDa and the cleaved and active form with a molecular size of 57 kDa, with the newly synthesized pro-form of the protein being the predominant cytosolic form under normal conditions. The protein is translocated into the mitochondria where the mitochondrial localization signal is cleaved, producing the smaller active form [19]. Our immunoblot analysis showed that the pro-form was indeed present in the cytosol of unchallenged MN9D cells, but also in the challenged cells. The cleaved form, however, was present mainly in the mitochondria (fig. 5A). Upon MPP^+ challenge, there was a significant increase in the cleaved form of AIF at the first 2 h of treatment. The change in AIF level in the cytosol was not due to an overall increase in protein synthesis since the increase was specifically for the cleaved form but not the pro-form. The increase in the cleaved form of AIF could be attributed to the release of the active protein from the mitochondria upon MPP^+ induction, since the formation of the active form requires cleavage of the mitochondrial localization signal in the mitochondria. As in the detection of cytochrome *c* release, none of the cytosolic fractions was positive for COXI, indicating that the AIF release was not due to membrane leakage during sample preparation (fig. 5A).

AIF has been reported to translocate to the nucleus to execute pro-apoptotic functions [19]. To test if AIF was indeed released and translocated to the nucleus upon MPP^+ challenge in this cell line, immunocytochemistry experiments were performed. Figure 5B shows the mitochondria staining and AIF localization in unchallenged MN9D cells. Superimposition of the two images showed that fluorescence staining of both the mitochondria and AIF

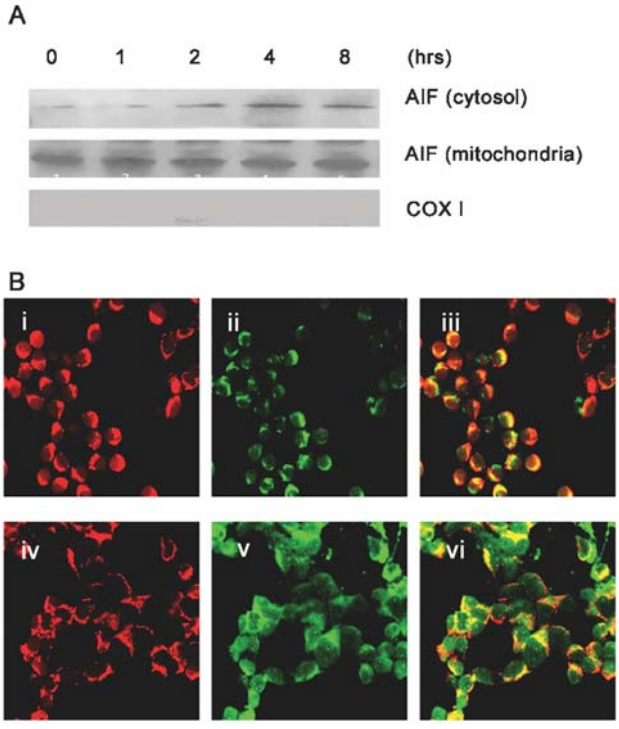

Figure 5. Localization of AIF in MN9D cells after neurotoxin treatment. MN9D cells were treated with 500 µM MPP^+. (*A*) At the time point indicated, cytosolic and mitochondrial fractions were harvested from the cell using ultracentrifugation. Proteins from these fractions were resolved using 12% SDS-PAGE, transferred to nitrocellulose and immunoblotted with AIF antibody. COXI was used to determine if there was membrane leakage. (*B*) Photomicrographs localizing AIF after MPP^+ treatment. MN9D cells were labeled with 250 nM Mitotracker red dye (Molecular Probes), AIF primary antibody (Santa Cruz) and FITC-conjugated anti-goat secondary antibody (Chemicon): i, mitochondria staining of unchallenged MN9D cells; ii, AIF localization of unchallenged MN9D cells; iii, superimposed image of i and ii; iv, mitochondria staining of MPP^+-challenged MN9D cells; v, AIF localization of MPP^+-challenged MN9D cells; vi, superimposed image of iv and v.

overlapped extensively with very little AIF staining outside the mitochondria. Figure 5 also shows the mitochondria staining and AIF localization, in MPP^+-challenged MN9D cells. AIF staining could be clearly seen outside the mitochondria, as well as within the nucleus area (fig. 5B). Thus, the exposure of MN9D cells to MPP^+ may have elicited the pro-apoptotic action of AIF by inducing its release from the mitochondria and mediating its translocation to the nucleus, causing chromatin condensation or DNA fragmentation that lead to cell death. Our finding is consistent with the in vivo observation of AIF translocation to the nucleus of TH-positive neurons in MPTP-treated mice [43].

Caspase-2, -8, -6 and -7 are activated in MPP^+-challenged MN9D cells

The lack of involvement of caspase-9 and caspase-3 led us to explore the caspase-independent cell death pathway. Phosphotidyl-inositol 3 kinase (PI3K) is a kinase upstream of Akt, which in turn signals a pro-survival pathway [44]. Wortmannin, an inhibitor of PI3K inhibits the phosphorylation of AKT, which negatively regulates apoptosis. Inhibition of AKT should thus lead to enhanced cell death. However, in MN9D cells, wortmannin did not significantly increase cell death (fig. 6A), suggesting that the caspase-independent pathway was not involved in the MPP^+-induced death mechanism of MN9D cells. The cell death in these cells could therefore involve the activation of other caspases which were investigated using inhibitors against initiator caspases such as caspase-2 and caspase-8. The application of caspase-2 inhibitor caused a partial rescue of the cells from MPP^+ challenge (fig. 6B). Significantly, caspase-8 inhibitor caused an almost complete rescue of the cells from MPP^+-induced cell death (fig. 6C). Thus, caspase-8 could be the major alternative initiator caspase. Since the final phase of apoptosis requires the action of effector caspases, and since caspase-3 has been demonstrated not to be activated in this model, the involvement of other effector caspases was subsequently tested. Our experiments showed that the introduction of caspase-6 inhibitor was able to rescue the cells from MPP^+ challenge (fig. 6D). In summary, this study points to some alternate cell death pathway(s) involving the initiator caspase-2, caspase-8, and effector caspase-6.

The sequential activation of caspases in MPP^+-induced cell death

The activation of caspases usually occurs as a cascade mechanism. For an insight into the sequence of caspase activation that took place in the MN9D cells upon MPP^+ challenge, a time-point study was conducted. MN9D cells were challenged with MPP^+ over a period of 1–24 h and immunoblots were first performed on these cell lysates to obtain the time of activation of various caspases. For the initiator caspases, such as caspase-2 and caspase-8, the cleaved forms of both caspases were evident from the first hour of MPP^+ challenge (Fig. 7A, B). The levels of cleaved forms of both caspases were markedly increased above that in the constitutively expressed unchallenged state. The cleaved forms were present at all the remaining time points, indicating that the activation of these caspases was maintained throughout MPP^+ challenge. Caspase-2 and caspase-8 were thus activated very early in the apoptotic cascade upon MPP^+ challenge. To test the activation of downstream effector caspases, the same experiment was performed against caspase-6 and caspase-7. The cleaved form of caspase-6 (15 kDa) only appeared from the second hour of MPP^+ challenge (fig. 7C), while the cleaved band of caspase-7 (20 kDa) appeared only from the eight hour of MPP^+ challenge (fig. 7D).

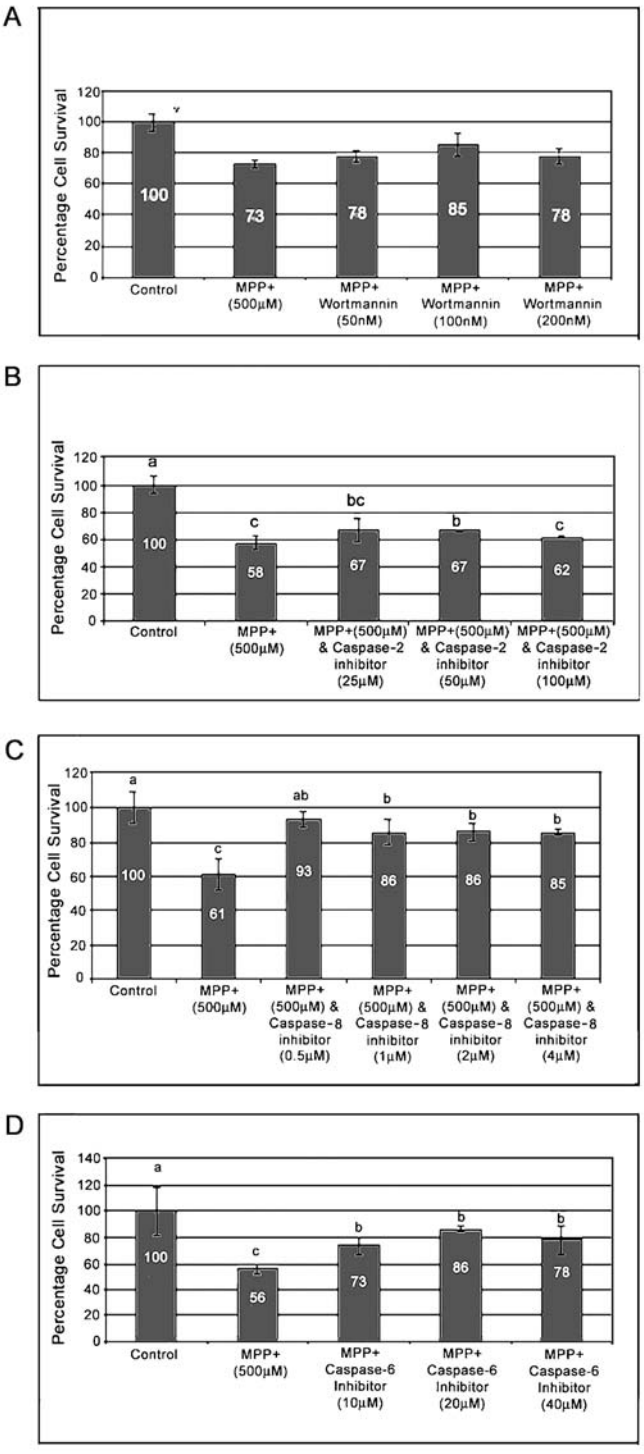

Figure 6. Percentage cell survival of MPP+-treated MN9D cells in the presence of PI3K and caspase inhibitors. Cells were treated with 500 μM MPP+ for 24 h in the presence of wortmannin (PI3K inhibitor) (*A*), caspase-2 inhibitor (*B*); caspase-8 inhibitor (*C*) and a caspase-6 inhibitor (*D*). Viability of cells was assayed using an MTT assay after treatment and was expressed as a percentage of control cells. Data represent the mean ± SE from three independent experiments (* $p < 0.05$).

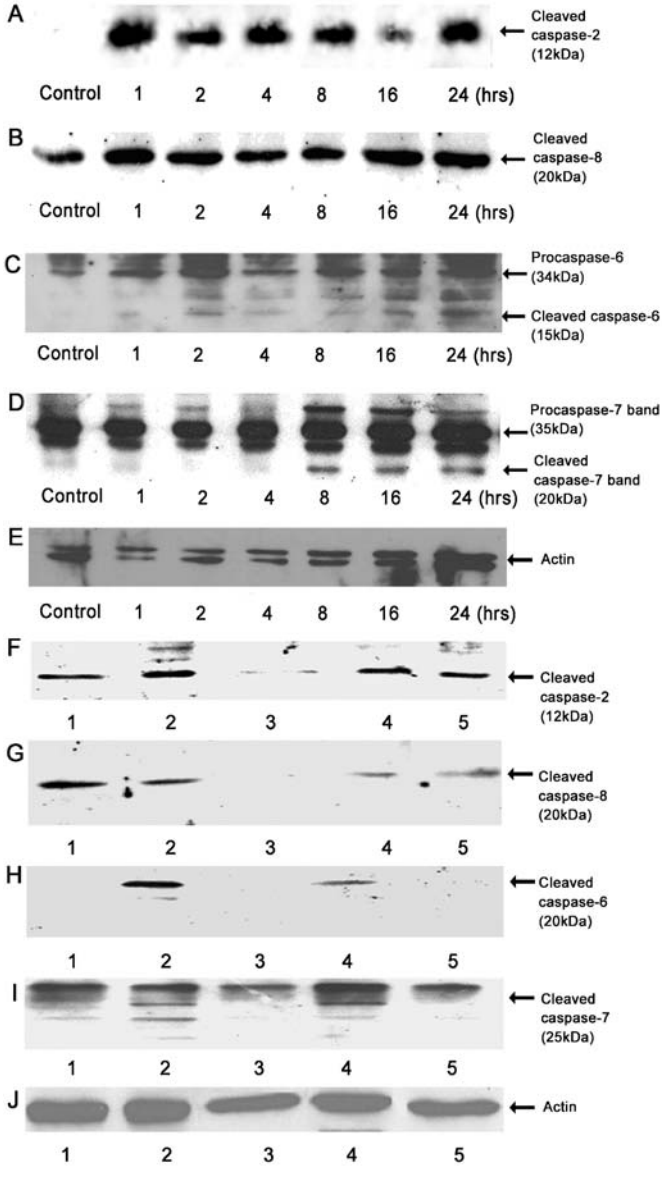

Figure 7. Caspase activation in MPP+-treated MN9D cells. Cell lysates were harvested from MN9D cells treated with 500 μM MPP+. Cytosolic proteins were separated by 12% SDS-PAGE and transferred to nitrocellulose membrane. (*A–D*) MN9D cells were treated with MPP+ for the time period indicated before detection of caspase-2, -8, -6 and -7 activation. (*F–I*) MN9D cells were treated with 500 μM MPP+ (lane 2) in the presence of inhibitors of caspase-2 (50 μM) (lane 3), caspase-6 (20 μM) (lane 4) and caspase-8 (20 μM) (lane 5) prior to Western blotting for activated caspase-2, -8, -6 and -7. (*E, J*) Actin probed to show equal loading of protein lysates in the gel.

To further confirm the order of sequential activation of caspases, inhibitors were used against the upstream caspases and immunoblots were used to test if the proposed downstream caspases could still be activated. Since the activation of the caspases was maintained throughout MPP+ challenge, only lysates of cells challenged with MPP+ for 24 h were used in order to facilitate this series

of experiments. Figure 7F shows that in the presence of caspase-2, -6 and -8 inhibitors, cleaved bands of caspase-2 were detected in all cell lysates of MPP^+-treated MN9D cells. When detection of cleaved caspase-8 was carried out on the cell lysates, it was only detected in the presence of both caspase-6 and -8 inhibitors but not when caspase-2 inhibitors were present (fig. 7G). In the presence of caspase-2 and -8 inhibitors, cleaved caspase-6 was not detected in these cell lysates (fig. 7H). Intriguingly, caspase-7 was detected in the presence of caspase-6 inhibitor but not caspase-2 and -8 inhibitors (fig. 7I), suggesting that caspase-7 might be of a similar hierarchy as caspase-6 in the MPP^+-induced apoptotic signaling cascade in MN9D cells. Taken together, the inhibition studies indicate an early activation of caspase-2 and caspase-8 upon MPP^+ challenge which is required for the subsequent activation of caspase-6 and caspase-7.

Discussion

Apoptosis is involved in the death of MPP^+-challenged MN9D cells

The mode of neuronal death in PD is still a subject of debate. In contrast to previous studies [31, 32], our results indicated the involvement of the apoptotic pathway in MPP^+-induced cell death in MN9D. We found no significant increase in LDH liberation by MPP^+-treated MN9D cells in comparison to the untreated cells, hence ruling out necrosis as a main mode of cell death that contributed to the overall cell loss. The discrepancies between previous results and ours may be attributed to the difference in dosage and duration of MPP^+ treatment used in the experiments. Choi et al. [31, 32] treated the cells with 25–100 μM MPP^+ over 12–36 h, while we applied the dosage of 500 μM MPP^+ under serum-free conditions over 24 h. To substantiate our claims, MPP^+-treated cells were stained with acridine orange/ethidium bromide and we detected a high percentage of chromatin condensation indicative of apoptosis (fig. 2B).

Blockage of the caspase-9/-3 apoptotic pathway

Despite constitutive activation of caspase-9 under serum-free conditions, the effector caspase-3 was not activated (fig. 3B). The failure of both caspase-9 and caspase-3 inhibitors to rescue MN9D cells challenged with MPP^+ affirmed the lack of their involvement in the cell death process (fig. 3 D, E). The caspase-9/3 pathway could have been inhibited as a result of MPP^+ treatment. XIAP has been shown to bind to activated caspase-9 and inhibit its activity [40, 41, 45]. The involvement of XIAP in this instance was tested by inhibiting its activation indirectly using the NF-κB inhibitor, SN50. SN50 blocks the activation of NF-κB by inhibiting its phosphorylation [42, 46]. As expected, the inhibition of NF-κB resulted in an increase in cell death (fig. 4). The depletion of ATP as a consequence of MPP^+ treatment [38] could have also contributed to such a phenomenon. The lack of caspase-3 activation in MPP^+-treated MN9D cells has also been reported recently in two separate studies [12, 24].

The ability of caspase-2 or caspase-8 inhibitor to rescue the cells implies the involvement of these caspases during MPP^+ challenge. These caspases belong to the initiator caspase group which is activated early during an apoptotic event, and our data demonstrated the early activation of caspase-2 and -8 in MN9D cells within the first hour of exposure to MPP^+. Here we speculate that MPP^+, a complex I inhibitor, caused the depletion of ATP in the MN9D cells, and since caspase-3 activation is ATP dependent, the cells then switched to activate alternate caspase-2, and/or -8, to elicit the apoptotic cell death. When ATP was added to the cytosolic fraction obtained from MPP^+-treated MN9D cells, caspase-3 was activated [12].

In the absence of caspase-3, caspase-6 might be activated as a compensatory mechanism for cells to proceed with the apoptotic cell death pathway. The activation of alternate compensatory caspases in cultured hepatocytes deficient in caspase-9 and caspase-3 has been reported [22]. The lack of caspase-9 and caspase-3 was shown to lead to the activation of other caspases such as caspase-2, -6 and -7 when cell death was induced with the Fas agonistic antibody, Jo2 [22]. The same compensatory activation of caspase-6 in caspase-3-deficient MCF7 cell line has also been demonstrated [47]. The MCF7 cell line was able to undergo apoptosis, when induced with the apoptosis stimulant Bax protein, despite the absence of caspase-3. Based on such studies, a similar scenario might be occurring in our cell model. Caspase-6 could indeed be the effector activated in MN9D cells as a compensation for the inactive caspase-3 upon MPP^+ challenge.

Alternate apoptotic pathway(s) involving caspase -2, -8, -6, and -7

Upon initiation of an apoptotic signal, hierarchical caspases are activated via proteolytic cascades in the cell. Our experiments revealed that when MN9D cells were treated with 500 μM MPP^+ for 24 h under serum-free conditions, both caspase-2 and -8 were activated in the first hour of challenge, followed by the activation of caspase-6 in the second hour and subsequently the activation of caspase-7 in the eight hour. To further verify this order of activation, specific inhibitors against the activated caspases were used to reaffirm their hierarchy in the MPP^+-induced apoptotic pathway. The inhibition studies further demonstrated that caspase-2 is the most upstream followed by caspase-8, while caspase-6 and -7 are downstream. Studies have demonstrated that caspase-2 is needed to induce the release of apoptotic factors from the mitochondria [48, 49]. Caspase-8 can then be activated

via apoptotic factors released from the mitochondria. The activation of caspase-6 and caspase-7 in the absence of caspase-3 activity comes as no surprise. These two downstream effector caspases are highly homologous to caspase-3 in their structure and substrate specificity [50]. Without caspase-3, both caspase-6 and caspase-7 have been demonstrated to bring about cell death via apoptosis. Caspase-6 can mediate nuclear shrinkage and nuclear fragmentation, bringing about nuclear apoptosis [51]. Caspase-7 also seems to be able to compensate for the lack of caspase-3 by bringing about extra-nuclear changes [52, 53].

Caspase-12 is known to be a specific sensor of endoplasmic reticulum (ER) stress [50]. While calpain and caspase-7 have been proposed to activate caspase-12 [54, 55], caspase-12 was proposed to mediate cytochrome *c*-independent activation of caspase-9 [56, 57]. On the other hand, mitochondria-released cytochrome *c* has been demonstrated to be able to translocate into the ER where it binds inositol (1, 4, 5) triphosphate receptors, leading to calcium release and amplifying the apoptotic signal [58]. In addition, a recent study showed that apoptosis induced by ER stress depends on activation of caspase-3 via caspase-12 [59]. In our experiments, caspase-3 was not activated by MPP^+ treatment. Akin to MPP^+, rotenone is also a neurotoxin that inhibits the mitochondrial complex 1. In our separate experiments that investigated the activation of caspases by rotenone treatment in MN9D cells, both casapse-3 and caspase-12 were not activated (unpublished data). A recent review on caspases involved in ER stress-mediated cell death highlighted that the level of caspase-12 expression is different in various mouse cells [60]. Taking the above considerations together, we do not think that caspase-12 is involved in the compensatory cell death pathway in MN9D cells challenged with MPP^+.

AIF is also involved in MN9D apoptosis

A critical step for apoptotic triggers effectiveness is the release of pro-apoptotic factors from the mitochondria. In our experiments, MPP^+ was found to induce increased release of cytochrome *c* and AIF from the mitochondria to the cytosol in the challenged MN9D cells. AIF has been demonstrated to activate both caspase-8 and caspase-3 [18], and cause chromatin condensation and large-scale DNA fragmentation, independent of caspase activation, upon release from the mitochondria [19]. Factors that could induce the release of AIF from the mitochondria include ATP depletion [61]. Our experiments demonstrated the migration of AIF from the mitochondria into the cytosol and the nucleus (fig. 5B) where it can potentially exert its apoptotic effect [19, 43]. Its concentration in the nucleus may cause apoptosis independent of Bax and caspases by inducing nuclear DNA damage [61]. Recent experiments in MPTP-treated animal models of PD have shown that excitotoxicity-induced neuronal death involved the translocation of AIF and PARP-mediated apoptosis [43]. We have also found an increase in PARP level in the MN9D cells after MPP^+ treatment (unpublished observation).

The activation of caspase-8 could also be due to the release of cytochrome *c*, although its actual mechanism is not well defined [62]. Caspase-6 has been demonstrated to be the direct activator of caspase-8 in cytochrome *c*-induced apoptosis in the human leukemic T cell line, Jurkat cells [21]. In our study, caspase-8 seems to be activated before caspase-6 although both activations occurred in the first 2 h after MPP^+ treatment. We cannot rule out the possibility that caspase-6 would act subsequently to cleave caspase-8, since complex feedback mechanisms of caspase processing are known to occur in apoptosis [63]. On the other hand, activated caspase-8 can activate Bid and then cause further cytochrome *c* release, thus reinforcing caspase activation [64, 65]. Apoptosis induction by caspase-8 has also been shown to amplify through cytochrome *c* [62]. In our experiments, increased cytochrome *c* release was observed within the first 2 h of MPP^+ treatment together with caspase-8 and caspase-6 activation. They are likely to mutually enhance each other to cause apoptosis. The involvement of caspase-8 in MN9D cell death is consistent with the findings of caspase-8 activation in a mouse PD model [14] and in human postmortem tissue [66].

In a recent study, caspase-3, -7, and -8 activation in the MN9D cells were observed 6 h after treatment with 6-OHDA [23]. Our study showed early activation of caspase-8 before caspase-7 in MPP^+-treated cells. The different orders of caspase activation could be due to the different neurotoxins used. MN9D cells subjected to 6-OHDA treatment have also been reported to die via a caspase-dependent pathway while MPP^+ treatment induced a caspase-independent pathway [12]. One of the explanations put forward was that MPP^+ may activate calpain in MN9D cells which may then prevent the entry into a caspase-dependent cell death by inhibiting the processing of procaspase-9 and procaspase-3 into their active subunits [12]. Here we show that while caspase-9 and -3 were not activated in the MN9D cells under 500 μM MPP^+ treatment, the cells did, however, die via apoptosis due to caspase-2, -8, -6, -7 and AIF.

Although our results may seem contradictory to others, they support the paradigm that the various caspase cascades induced by apoptotic stimuli are rather flexible in nature, and that alternate compensatory caspase cascades may be activated to mediate apoptotic cell death, as demonstrated by Zheng et al. [22]. Degterev et al [50] have also reviewed the paradox that none of the downstream effector capases acting as executioners seem to fully control all the aspects of apoptosis. Redundancy and compensatory networks in case ‘primary’ caspases are missing may well be at work in most cells. Of interest will

be to further investigate if such compensatory mechanisms observed in MN9D cells are conserved across other dopaminergic cells including those in the mouse ventral midbrain or even in PD tissues.

Acknowledgements. We thank Dr A. Heller, University of Chicago, for permission to use the MN9D cells. We also thank Dr K. L. Chua, Department of Biochemistry, NUS, for critical review of this manuscript. This work was supported by a program grant from the Biomedical Research Council, Agency for Science, Technology and Research, Singapore.

1 Dauer W. and Przedborski S. (2003) Parkinson's disease: mechanisms and models. Neuron **39:** 889–909
2 Dawson T. M. and Dawson V. L. (2003) Molecular pathways of neurodegeneration in Parkinson's disease. Science **302:** 819–822
3 Lim K. L. and Lim T. M. (2003) Molecular mechanisms of neurodegeneration in Parkinson's disease: clues from Mendelian syndromes. IUBMB Life **55:** 315–322
4 Hartmann A., Hunot S., Michel P. P., Muriel M. P., Vyas S., Faucheux B. A. et al. (2000) Caspase-3: a vulnerability factor and final effector in apoptotic death of dopaminergic neurons in Parkinson's disease. Proc. Natl. Acad. Sci. USA **97:** 2875–2880
5 Blum D., Torch S., Lambeng N., Nissou M., Benabid A. L., Sadoul R. et al. (2001) Molecular pathways involved in the neurotoxicity of 6-OHDA, dopamine and MPTP: contribution to the apoptotic theory in Parkinson's disease. Prog. Neurobiol. **65:** 135–172
6 Barzilai A. and Melamed E. (2003) Molecular mechanisms of selective dopaminergic neuronal death in Parkinson's disease. Trends Mol. Med. **9:** 126–132
7 Fiskum G., Starkov A., Polster B. M. and Chinopoulos C. (2003) Mitochondrial mechanisms of neural cell death and neuroprotective interventions in Parkinson's disease. Ann. N. Y. Acad. Sci. **991:** 111–119
8 Liou A. K., Clark R. S., Henshall D. C., Yin X. M. and Chen J. (2003) To die or not to die for neurons in ischemia, traumatic brain injury and epilepsy: a review on the stress-activated signaling pathways and apoptotic pathways. Prog. Neurobiol. **69:** 103–142
9 Tatton W. G., Chalmers-Redman R., Brown D. and Tatton N. (2003) Apoptosis in Parkinson's disease: signals for neuronal degradation. Ann Neurol **53 (suppl 3):** S61–70; discussion S70–72
10 Mochizuki H., Goto K., Mori H. and Mizuno Y. (1996) Histochemical detection of apoptosis in Parkinson's disease. J. Neurol. Sci. **137:** 120–123
11 Kingsbury A. E., Mardsen C. D. and Foster O. J. (1998) DNA fragmentation in human substantia nigra: apoptosis or perimortem effect? Mov. Disord. **13:** 877–884
12 Han B. S., Hong H. S., Choi W. S., Markelonis G. J., Oh T. H. and Oh Y. J. (2003) Caspase-dependent and -independent cell death pathways in primary cultures of mesencephalic dopaminergic neurons after neurotoxin treatment. J. Neurosci. **23:** 5069–5078
13 Viswanath V., Wu Z., Fonck C., Wei Q., Boonplueang R. and Andersen J. K. (2000) Transgenic mice neuronally expressing baculoviral p35 are resistant to diverse types of induced apoptosis, including seizure-associated neurodegeneration. Proc. Natl. Acad. Sci. USA **97:** 2270–2275
14 Viswanath V., Wu Y., Boonplueang R., Chen S., Stevenson F. F., Yantiri F. et al. (2001) Caspase-9 activation results in downstream caspase-8 activation and bid cleavage in 1-methyl-4-phenyl-1,2,3,6-tetrahydropyridine-induced Parkinson's disease. J. Neurosci. **21:** 9519–9528
15 Green D. R. and Reed J. C. (1998) Mitochondria and apoptosis. Science **281:** 1309–1312
16 Li P., Nijhawan D., Budihardjo I., Srinivasula S. M., Ahmad M., Alnemri E. S. et al. (1997) Cytochrome c and dATP-dependent formation of Apaf-1/caspase-9 complex initiates an apoptotic protease cascade. Cell **91:** 479–489
17 Friberg H. and Wieloch T. (2002) Mitochondrial permeability transition in acute neurodegeneration. Biochimie **84:** 241–250
18 Fulda S., Susin S. A., Kroemer G. and Debatin K. M. (1998) Molecular ordering of apoptosis induced by anticancer drugs in neuroblastoma cells. Cancer Res. **58:** 4453–4460
19 Susin S. A., Lorenzo H. K., Zamzami N., Marzo I., Snow B. E., Brothers G. M. et al. (1999) Molecular characterization of mitochondrial apoptosis-inducing factor. Nature **397:** 441–446
20 Fiskum G. (2000) Mitochondrial participation in ischemic and traumatic neural cell death. J. Neurotrauma **17:** 843–855
21 Cowling V. and Downward J. (2002) Caspase-6 is the direct activator of caspase-8 in the cytochrome c-induced apoptosis pathway: absolute requirement for removal of caspase-6 prodomain. Cell Death Differ. **9:** 1046–1056
22 Zheng T. S., Hunot S., Kuida K., Momoi T., Srinivasan A., Nicholson D. W. et al. (2000) Deficiency in caspase-9 or caspase-3 induces compensatory caspase activation. Nat. Med. **6:** 1241–1247
23 Choi W. S., Eom D. S., Han B. S., Kim W. K., Han B. H., Choi E. J. et al. (2004) Phosphorylation of p38 MAPK induced by oxidative stress is linked to activation of both caspase-8- and -9-mediated apoptotic pathways in dopaminergic neurons. J. Biol. Chem. **279:** 20451–20460
24 Holtz W. A. and O'Malley K. L. (2003) Parkinsonian mimetics induce aspects of unfolded protein response in death of dopaminergic neurons. J. Biol. Chem. **278:** 19367–19377
25 Choi H. K., Won L. A., Kontur P. J., Hammond D. N., Fox A. P., Wainer B. H. et al. (1991) Immortalization of embryonic mesencephalic dopaminergic neurons by somatic cell fusion. Brain Res **552:** 67–76
26 Choi H. K., Won L., Roback J. D., Wainer B. H. and Heller A. (1992) Specific modulation of dopamine expression in neuronal hybrid cells by primary cells from different brain regions. Proc. Natl. Acad. Sci. USA **89:** 8943–8947
27 Davis G. C., Williams A. C., Markey S. P., Ebert M. H., Caine E. D., Reichert C. M. et al. (1979) Chronic Parkinsonism secondary to intravenous injection of meperidine analogues. Psychiatry Res. **1:** 249–254
28 Zhang W. D., Wen Y., Liu S. M., Tjiu W. C., Xu G. Q. and Gan L. M. (2002) Synthesis of vertically aligned carbon nanotubes on metal deposited quartz plates. Carbon **40:** 1981–1989
29 Smedes F., Kraak J. C. and Poppe H. (1982) Simple and fast solvent extraction system for selective and quantitative isolation of adrenaline, noradrenaline and dopamine from plasma and urine. J. Chromatogr. **231:** 25–39
30 Tang L., Todd R. D. and O'Malley K. L. (1994) Dopamine D2 and D3 receptors inhibit dopamine release. J. Pharmacol. Exp. Ther. **270:** 475–479
31 Choi W. S., Yoon S. Y., Oh T. H., Choi E. J., O'Malley K. L. and Oh Y. J. (1999) Two distinct mechanisms are involved in 6-hydroxydopamine- and MPP^+-induced dopaminergic neuronal cell death: role of caspases, ROS, and JNK. J. Neurosci. Res **57:** 86–94
32 Choi W. S., Canzoniero L. M., Sensi S. L., O'Malley K. L., Gwag B. J., Sohn S. et al. (1999) Characterization of MPP(+)-induced cell death in a dopaminergic neuronal cell line: role of macromolecule synthesis, cytosolic calcium, caspase, and Bcl-2-related proteins. Exp. Neurol. **159:** 274–282
33 Oh J. H., O'Malley K. L., Krajewski S., Reed J. C. and Oh Y. J. (1997) Bax accelerates staurosporine-induced but suppresses nigericin-induced neuronal cell death. Neuroreport **8:** 1851–1856

34 Oh Y. J., Uhland-Smith A., Kim J. E. and O'Malley K. L. (1997) Regions outside of the Bcl-2 homology domains, BH1 and BH2 protect a dopaminergic neuronal cell line from staurosporine-induced cell death. Brain Res. Mol. Brain Res. **51:** 133–142
35 Oh J. H., Choi W. S., Kim J. E., Seo J. W., O'Malley K. L. and Oh Y. J. (1998) Overexpression of HA-Bax but not Bcl-2 or Bcl-XL attenuates 6-hydroxydopamine-induced neuronal apoptosis. Exp. Neurol. **154:** 193–198
36 Perez R. G., Waymire J. C., Lin E., Liu J. J., Guo F. and Zigmond M. J. (2002) A role for alpha-synuclein in the regulation of dopamine biosynthesis. J. Neurosci. **22:** 3090–3099
37 Nicklas W. J., Vyas I. and Heikkila R. E. (1985) Inhibition of NADH-linked oxidation in brain mitochondria by 1-methyl-4-phenyl-pyridine, a metabolite of the neurotoxin, 1-methyl-4-phenyl-1,2,5,6-tetrahydropyridine. Life Sci. **36:** 2503–2508
38 Mizuno Y., Sone N., Suzuki K. and Saitoh T. (1988) Studies on the toxicity of 1-methyl-4-phenylpyridinium ion (MPP^+) against mitochondria of mouse brain. J. Neurol. Sci. **86:** 97–110
39 Cassarino D. S., Parks J. K., Parker W. D., Jr. and Bennett J. P., Jr. (1999) The parkinsonian neurotoxin MPP+ opens the mitochondrial permeability transition pore and releases cytochrome c in isolated mitochondria via an oxidative mechanism. Biochim Biophys. Acta **1453:** 49–62
40 Srinivasula S. M., Hegde R., Saleh A., Datta P., Shiozaki E., Chai J. et al. (2001) A conserved XIAP-interaction motif in caspase-9 and Smac/DIABLO regulates caspase activity and apoptosis. Nature **410:** 112–116
41 Deveraux Q. L. and Reed J. C. (1999) IAP family proteins – suppressors of apoptosis. Genes Dev. **13:** 239–252
42 Xiao C. W., Ash K. and Tsang B. K. (2001) Nuclear factor-kappaB-mediated X-linked inhibitor of apoptosis protein expression prevents rat granulosa cells from tumor necrosis factor alpha-induced apoptosis. Endocrinology **142:** 557–563
43 Wang H., Shimoji M., Yu S. W., Dawson T. M. and Dawson V. L. (2003) Apoptosis inducing factor and PARP-mediated injury in the MPTP mouse model of Parkinson's disease. Ann. N. Y. Acad. Sci. **991:** 132–139
44 Brunet A., Bonni A., Zigmond M. J., Lin M. Z., Juo P., Hu L. S. et al. (1999) Akt promotes cell survival by phosphorylating and inhibiting a Forkhead transcription factor. Cell **96:** 857–868
45 Sun C., Cai M., Meadows R. P., Xu N., Gunasekera A. H., Herrmann J. et al. (2000) NMR structure and mutagenesis of the third Bir domain of the inhibitor of apoptosis protein XIAP. J. Biol. Chem. **275:** 33777–33781
46 Zhang Y., Dawson V. L. and Dawson T. M. (2000) Oxidative stress and genetics in the pathogenesis of Parkinson's disease. Neurobiol. Dis. **7:** 240–250
47 Kagawa S., Gu J., Honda T., McDonnell T. J., Swisher S. G., Roth J. A. et al. (2001) Deficiency of caspase-3 in MCF7 cells blocks Bax-mediated nuclear fragmentation but not cell death. Clin. Cancer Res. **7:** 1474–1480
48 Lassus P., Opitz-Araya X. and Lazebnik Y. (2002) Requirement for caspase–2 in stress-induced apoptosis before mitochondrial permeabilization. Science **297:** 1352–1354
49 Guo Y., Srinivasula S. M., Druilhe A., Fernandes-Alnemri T. and Alnemri E. S. (2002) Caspase-2 induces apoptosis by releasing proapoptotic proteins from mitochondria. J. Biol. Chem. **277:** 13430–13437
50 Degterev A., Boyce M. and Yuan J. (2003) A decade of caspases. Oncogene **22:** 8543–8567
51 Hirata H., Takahashi A., Kobayashi S., Yonehara S., Sawai H., Okazaki T. et al. (1998) Caspases are activated in a branched protease cascade and control distinct downstream processes in Fas-induced apoptosis. J. Exp. Med. **187:** 587–600
52 Talanian R. V., Quinlan C., Trautz S., Hackett M. C., Mankovich J. A., Banach D. et al. (1997) Substrate specificities of caspase family proteases. J. Biol. Chem. **272:** 9677–9682
53 Thornberry N. A., Rano T. A., Peterson E. P., Rasper D. M., Timkey T., Garcia-Calvo M. et al. (1997) A combinatorial approach defines specificities of members of the caspase family and granzyme B: functional relationships established for key mediators of apoptosis. J. Biol. Chem. **272:** 17907–17911
54 Nakagawa T. and Yuan J. (2000) Cross-talk between two cysteine protease families: activation of caspase-12 by calpain in apoptosis. J. Cell. Biol. **150:** 859–854
55 Rao R. V., Hermel E., Castro-Obregon S., Rio G. del Ellerby L. M., Ellerby H. M. et al. (2001) Coupling endoplasmic reticulum stress to the cell death program. Mechanism of caspase activation. J. Biol. Chem. **276:** 33869–33874
56 Morishima N., Nakanishi K., Takenouchi H., Shibata T. and Yasuhiko Y. (2002) An endoplasmic reticulum stress-specific caspase cascade in apoptosis: cytochrome c-independent activation of caspase-9 by caspase-12. J. Biol. Chem. **277:** 34287–34294
57 Rao R. V., Castro-Obregon S., Frankowski H., Schuler M., Stoka V., del Rio G. et al. (2002) Coupling endoplasmic reticulum stress to the cell death program: an Apaf-1-independent intrinsic pathway. J. Biol. Chem. **277:** 21836–21842
58 Boehning D, Patterson R. L., Sedaghat L., Glebova N. O., Kurosaki T. and Snyder S. H**.** (2003) Cytochrome c binds to inositol (1,4,5) trisphosphate receptors, amplifying calcium-dependent apoptosis. Nat. Cell. Biol. **5:** 1051–1061
59 Hitomi J., Katayama T., Taniguchi M., Honda A., Imaizumi K., and Tohyama M. (2003) Apoptosis induced by endoplasmic reticulum stress depends on activation of caspase-3 via caspase-12. Neurosci. Lett. **357:** 127–130
60 Momoi T. (2004) Caspases involved in ER stress-mediated cell death. J. Chem. Neuro. **28:** 101–105
61 Daugas E., Susin S. A., Zamzami N., Ferri K. F., Irinopoulou T., Larochette N. et al. (2000) Mitochondrio-nuclear translocation of AIF in apoptosis and necrosis. FASEB J. **14:** 729–739
62 Kuwana T., Smith J. J., Muzio M., Dixit V., Newmeyer D. D. and Kornbluth S. (1998) Apoptosis induction by caspase-8 is amplified through the mitochondrial release of cytochrome c. J. Biol. Chem. **273:** 16589–16594
63 Srinivasula S. M., Ahmad M., Fernandes-Alnemri T. and Alnemri E. S. (1998) Autoactivation of procaspase-9 by Apaf-1-mediated oligomerization. Mol. Cell. **1:** 949–957
64 Li H., Zhu H., Xu C. J. and Yuan J. (1998) Cleavage of BID by caspase 8 mediates the mitochondrial damage in the Fas pathway of apoptosis. Cell **94:** 491–501
65 Luo X., Budihardjo I., Zou H., Slaughter C. and Wang X. (1998) Bid, a Bcl2 interacting protein, mediates cytochrome c release from mitochondria in response to activation of cell surface death receptors. Cell **94:** 481–490
66 Hartmann A., Troadec J. D., Hunot S., Kikly K., Faucheux B. A., Mouatt-Prigent A. et al. (2001) Caspase-8 is an effector in apoptotic death of dopaminergic neurons in Parkinson's disease, but pathway inhibition results in neuronal necrosis. J. Neurosci. **21:** 2247–2255